Slip Distribution of the 2011 Tohoku-oki Earthquake

Yuichiro Tanioka
Professor, Institute of Seismology and Volcanology, Hokkaido University
E-mail: tanioka@mail.sci.hokudai.ac.jp

Aditya R Gusman
Post-doctal researcher, Institute of Seismology and Volcanology, Hokkaido University

Abstract

The slip distribution of the 11 March 2011 Tohoku earthquake is inferred from tsunami waveforms, GPS data, and seafloor crustal deformation data. The major slip region extends all the way to the trench, and the large slip area extends 250 km long and 160 km wide. The largest slip of 48 m is located up-dip of the hypocenter. The large slip amount, about 42 m, is estimated the plate interface near the trench. The seismic moment calculated from the estimated slip distribution is 5.3 × 10^{22} N m (Mw 9.1). The large tsunami due to the 2011 Tohoku earthquake is generated from that large slip area near the trench. The additional uplift at the sedimentary wedge as suggested for the 1896 Sanriku earthquake may occur during the 2011 Tohoku earthquake, too.

1. INTRODUCTION

The great 2011 Tohoku earthquake occurred on 11 March 2011 at 5:46:18 UTC with epicenter at 38.104° N and 142.861° E off the east coast of Tohoku and about 130 km from Sendai, Japan, according to the Japan Meteorological Agency (JMA). The largest foreshock occurred at 2:45:13 UTC on 9 March 2011 with Mw 7.3 (JMA) at 38.328° N and 143.28° E. The largest aftershock with Mw 7.7 occurred approximately 28 minutes after the mainshock (6:15:34 UTC) at 36.108° N and 141.265° E (JMA). Approximately 39 minutes after the mainshock (6:25:44 UTC) the largest outer-rise aftershock with a normal faulting geometry occurred with Mw 7.5 at 37.837° N and 144.894° E (JMA). Fig.1 shows the location of the mainshock, foreshocks and aftershocks.

The Global Centroid Moment Tensor (GCMT) solution estimated that the 2011 Tohoku earthquake released seismic moment of 5.3 × 10^{22} N m (Mw 9.1). The dip angle at the Centroid is ranging from 10° to 14° (GCMT, WCMT, and USGS). A rupture model of the 2011 earthquake by *Ammon et al.* [2011] included a low initial rupture speed (1.5 km/s) near the hypocenter and an increase in speed (2.5 km/s) at distances larger than 100 km from the hypocenter.

The 2011 Tohoku earthquake occurred within the Japan Trench subduction zone where the Pacific plate subducts beneath the Okhotsk plate. A large tsunami was generated by the 2011 Tohoku megathrust earthquake and devastated the coastal area along the north east coast of Honshu. The National Police Agency of Japan has confirmed casualties of about 16,000 deaths, 4,000 people missing, and 6,000 injured. The tsunami was observed by tide gauges, pressure gauges, GPS buoys,

and Deep-ocean Assessment and Reporting of Tsunamis (DART) buoys that are located offshore and across the Pacific Ocean.

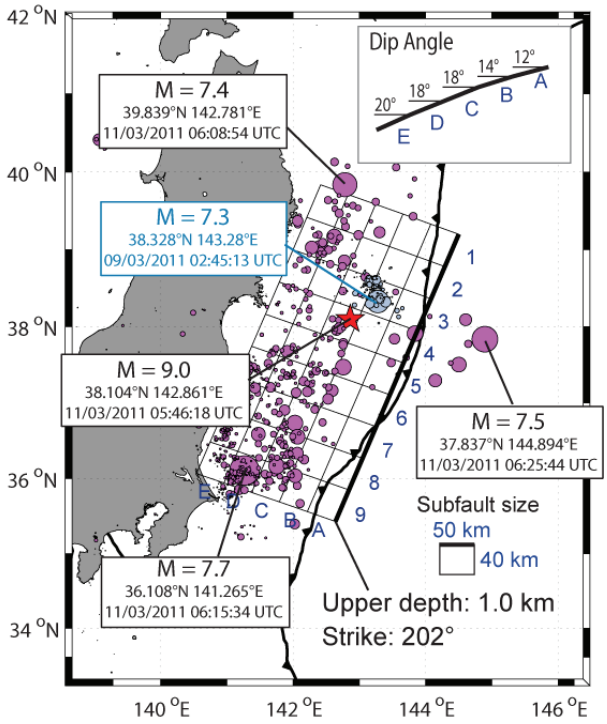

Fig. 1: Map of the 2011 Tohoku earthquake. Red star represents the epicenter of the mainshock, gray circles represent foreshocks and purple circles represent aftershocks.

A dense Global Positioning System (GPS) network of the Earth Observation Network (GEONET) on main islands of Japan that is maintained by Geospatial Information Authority of Japan (GSI) [*Sagiya et al.*, 2000] detected coseismic and postseismic displacements due to the 2011 earthquake [*Ozawa et al.*, 2011]. Crustal movement monitoring at underwater reference stations off the east coast of Tohoku reveals that coseismic displacement there due to the earthquake are large up to 24 m of horizontal motion [*Sato et al.*, 2011].

Previous studies indicated that large slip beneath a sedimentary wedge near the trench caused large horizontal movement of backstop and that generated large additional uplift of the sediment [*Seno*, 2000; *Tanioka and Seno*, 2001; *Seno and Hirata*, 2007]. Those studies indicated that this additional uplift of sediment near a trench has large effect on tsunami generation. The uplift of sediments near the trench can be calculated from the horizontal movement of the backstop [*Tanioka and Seno*, 2001].

In this paper, we estimate the source model of the 2011 great Tohoku earthquake using tsunami waveforms, GPS data on main Islands of Japan and seafloor crustal deformation data.

2. OBSERVATION DATA

2.1 Tsunami Waveforms

To estimate slip distribution of the earthquake, we use tsunami waveforms at 17 stations **(**Fig.2). These stations include 5 DART buoys in the Pacific Ocean (DART21401, DART21413, DART21418, DART21419 and DART52402), 4 tide gauges in Japan, (Erimo, Mori, Katsuura, and Ito), 2 bottom-pressure gauges off the coast of Tokachi (KPG1 and KPG2), 2 bottom-pressure gauges off the coast of Iwate (TM1 and TM2), and 4 GPS buoys off the coast of Iwate, Miyagi, and Fukushima (GPSB802, GPSB803, GPSB804 and GPSB806).

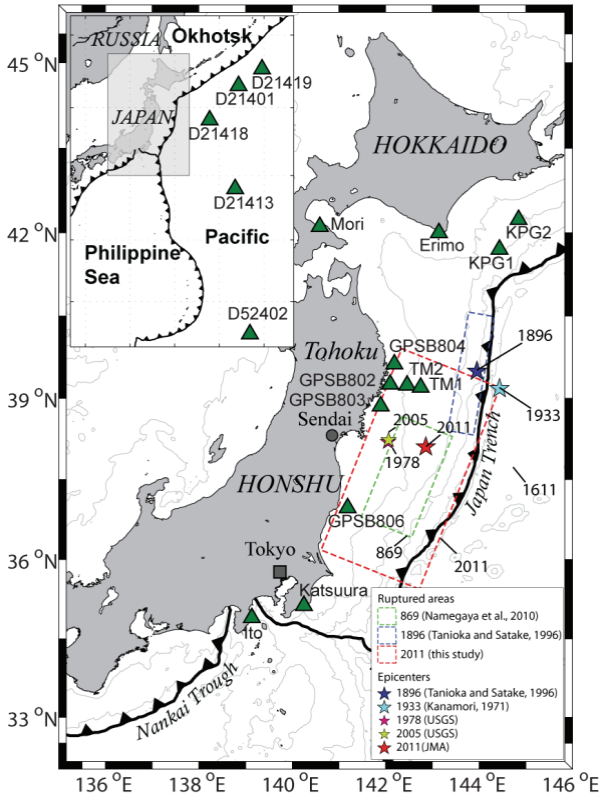

Fig.2: Map of sea level observation stations (green triangles). Stars represent epicenters and rectangles represent ruptured areas.

These tide gauge and buoy records include ocean tides, which are needed to be removed to get the tsunami waveforms. The ocean tides are approximated by fitting a polynomial function, and are removed from the original records. The records from the 4 bottom-pressure sensors (KPG1, KPG2,

TM1 and TM2) also include high frequency waves, the tsunami waveforms are approximated by calculating the moving average of the record.

2.2 Crustal Deformation Data

Crustal deformation due to the 2011 Tohoku earthquake was observed by the GPS GEONET that is operated by the GSI. The ARIA team at Jet Propulsion Laboratory (JPL) and California Institute of Technology (Caltech) estimated coseismic displacements due to the earthquake from 5 minutes interval of kinematic solutions of the GPS data. We use the coseismic displacements data estimated by the ARIA team at 1230 GPS stations in Japan to help estimate the slip distribution of the 2011 Tohoku Earthquake.

Crustal deformation on the seafloor above the hypocenter of the 2011 earthquake has been measured using a technique that combines GPS and acoustic technologies at 5 seafloor reference points (KAMS, KAMN, MYGI MYGW and FUKU) (**Figure 3a**). Displacements at the reference points due to mainshock, foreshocks and aftershocks of the 2011 earthquake until about 20 days after the mainshock are 5 to 24 m toward ESE and -8 to 3 upward [*Sato et al.*, 2011]. Displacements due to effects other than the mainshock are estimated to be not larger than 1 m, therefore, the recorded displacements are considered as the coseismic displacements [*Sato et al.*, 2011].

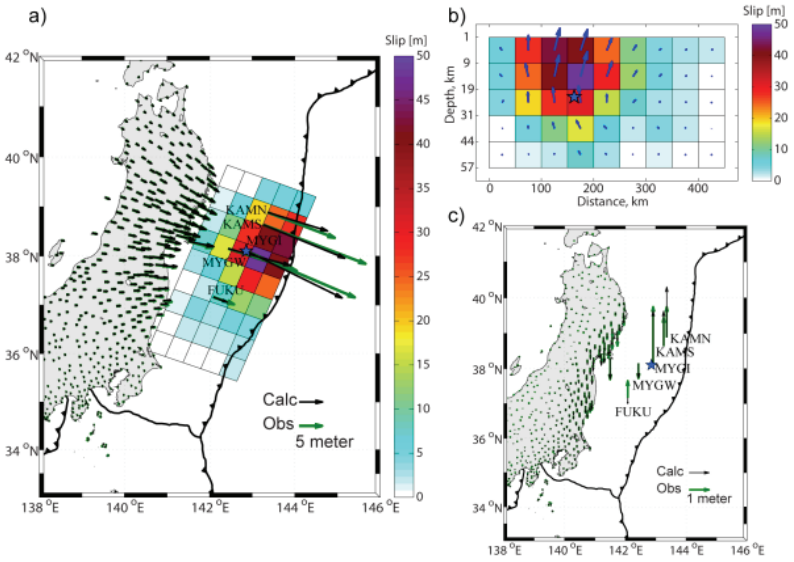

Fig. 3: a) Slip distribution of the 2011 Tohoku earthquake estimated from tsunami waveforms and crustal deformation data. Blue star represents the epicenter, green arrows and black arrows represent observed and calculated horizontal coseismic displacements, respectively. b) Slip distribution along strike, blue arrows represent rake angles on every subfault, blue star represents the hypocenter. c) Comparison between observed and calculated vertical coseismic displacements.

3. JOINT INVERSION OF TSUNAMI WAVEFORMS AND COSEISMIC DEFORMATION DATA

3.1 Tsunami Numerical Simulation

The bathymetry data sets used for tsunami simulation are based upon the General Bathymetric Chart of the Oceans (GEBCO) 30 arc-second data set and the Japan Hydrographic Association's M7001 and M7002 bathymetric contour data sets. The computation area ranges from 130° to 160° E and from 10° to 50° N. We use different grid systems with grid sizes of 90 arc-seconds, 30 arc-seconds, and 10 arc-seconds to compute the tsunami. The finest grids are used for the coastal area around the Erimo, Mori, Katsuura, and Ito tide gauge stations.

Synthetic tsunami waveforms generated from all subfaults at the stations were numerically computed by solving the linear shallow water equations with spherical coordinate system [*Johnson*, 1999]. Tsunami on the deep ocean is not affected by coastal effects, simulation of the tsunami using the linear shallow water equations is widely accepted [*Synolakis et al.*, 2008] The sea level observation instruments used different sampling rates, so the tsunami waveforms are resampled at 1 min interval and the synthetic tsunami waveforms are also resampled at 1 min interval.

3.2 Fault Parameters and Inversion

A ruptured plate interface is assumed to have a size with a length of 450 km and a width of 200 km by referring to aftershock distribution. Then the plate interface is divided into 45 subfaults with length and width of 50 km and 40 km, respectively. Strike for each subfault is assumed to be 202°, dip angles of 12°, 14°, 18°, 18° and 20° are used for the subfaults at depth of 1 km, 9 km, 19 km, 31 km and 44 km respectively (Fig.1). Rake angles of 45° and 135° are used for each subfault to estimate the slip direction of each subfault (within the range between 45° and 135°).

The initial sea surface deformation is assumed to be the same as the ocean bottom deformation if the spatial wavelength of the ocean bottom deformation is much larger than the ocean depth [*Satake*, 2002]. This assumption cannot be applied to obtain sea surface deformation from the ocean bottom deformation that is induced by faulting of a very shallow fault near a trench, because the deformation near the trench has steep slope with spatial wavelength that is smaller than ocean depth. Therefore, the initial sea surface deformation for subfaults near the trench (A and B subfaults) (Fig.1) is computed from the coseismic vertical deformation on the ocean bottom using *Kajiura* [1963] formula. For the other subfaults, it is assumed to be equal to the coseismic vertical deformation. The deformation on the ocean bottom is computed for each subfault with unit amount of slip using *Okada* [1985] formula.

We used non-negative least square method [*Lawson and Hanson*, 1974] and include a spatial smoothness constraint to estimate the slip distribution of the earthquake. The optimal value of smoothing factor was selected to minimize Akaike's Bayesian information criterion (ABIC) [*Akaike*, 1980]. For more details of our inversion method, see *Gusman et al*. [2010].

4. RESULTS

The maximum slip amount is estimated to be 48 m and the major slip region is located up-dip of the hypocenter with dimensions of roughly 250 km long and 160 km wide (Fig.3a). The earthquake ruptured the plate interface from the hypocenter all the way to the trench with large slip amount, about

42 m, near the trench. The seismic moment calculated from estimated slip distribution is 5.3×10^{22} N m (Mw 9.1) by assuming the rigidity of 4×10^{10} N m^{-2}. The estimated average rake angle from the slip distribution is 84° (Fig.3b). The slip distribution generated sea surface deformation with a maximum water level of 11 m above mean sea level.

The calculated horizontal and vertical displacements at GPS stations and at seafloor reference points resemble the observations. Comparisons between the calculated and the observed horizontal and vertical displacements are shown in Fig.3a and 3c. We compare the simulated tsunami waveforms from the estimated slip distribution with the observed tsunami waveforms at sea level observation stations in Fig.4. Overall, observed tsunami waveforms are well explained by simulated tsunami waveforms. However, small discrepancies of about 2 m between the observed and simulated tsunami waveforms remain at the stations near the tsunami source area (TM1, TM2, GPSB802, GPSB803, and GPSB804). We discuss this discrepancies further in the next section.

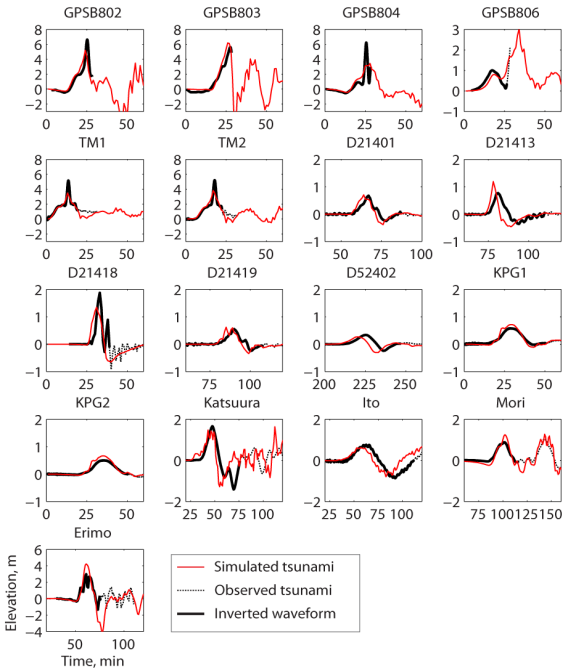

Fig. 4: Comparison of observed and simulated tsunami wave forms from the estimated slip distribution.

5. DISCUSSION

Because Tanioka and Seno [2001] suggested that the additional uplift along the unconsolidated sedimental wedge near the trench generated the additional tsunami for the 1896 Sanriku tsunmai, we also need to test that the small discrepancies between the observed and simulated tsunami waveforms at offshore stations near the source area of the 2011 earthquake can be explained by the additional

uplift near the trench. In this study, the calculation of the additional uplift is followed by Model A in Tanioka and Seno [2001],

To calculate additional uplift, we assume that the dip angle of the backstop slope (θ) is 50°, which is the same as Tanioka and Seno [2001], and the width of uplift area is 1.5 km. The horizontal movement (u_h) is calculated from the slip distribution inferred from tsunami waveforms and crustal deformation data.

The largest horizontal displacement near the trench is about 30 m which induced about 35 m of additional uplift. The sea surface deformation due of the additional uplift is calculated by the *Kajiura* [1963] formula because the width of the additional uplift is 1.5 km which is smaller than the ocean depth. Simulated tsunami waveforms from the slip distribution with additional uplift at stations near the source area (GPSB802, TM1 and TM2) better match the observed tsunami waveforms than those derived from only the slip distribution (Fig.4 and 5). The fits between observed and simulated tsunami waveforms at other stations from the source model including additional uplift are slightly worse than those from only the slip distribution because we add some uplifts to the tsunami initial condition computed from the result of the inversion. However, the differences are not significant. This suggests that the additional uplift as the same as the 1896 Sanriku tsunami earthquake may occurred during the 2011 great Tohoku earthquake because the 2011 Tohoku earthquake also ruptured the plate interface near the Japan Trench.

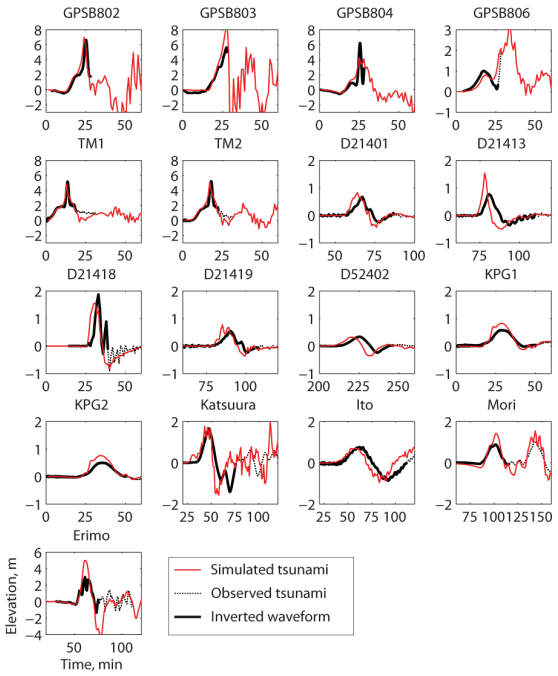

Fig. 5: Comparison of observed and simulated tsunami wave forms from the slip distribution with the additional uplift.

6. CONCLUSIONS

In this study, joint inversion is performed using tsunami waveforms, GPS data and seafloor deformation data to study the source model of the 2011 tsunami. The inferred slip distribution has a major slip region with the maximum slip amount of 48 m (Fig.3). The earthquake ruptured the plate interface from the hypocenter all the way to the trench with large slip amounts up to 42 m on the shallowest subfaults. The total seismic moment calculated from estimated slip distribution is 5.3×10^{22} N m (Mw 9.1) which is equal to that estimated by GCMT (5.3×10^{22} N m).

We indicate that not only coseismic vertical deformation, but also additional uplift near the trench as suggested for the 1896 Sanriku tsunami earthquake may contribute the large tsunami near the source of the 2011 Tohoku earthquake.

7. REFERENCES

[1] Akaike, H. (1980), Likelihood and the Bayes procedure, in *Bayesian Statistics*, edited by J. M. Bernando et al., pp. 143-166, Univ. Press, Valencia, Spain.

[2] Ammon, C. J., T. Lay, H. Kanamori, and M. Cleveland (2011), Preliminary rupture model of the great 2011 Tohoku-oki earthquake, *Earth Planets Space*, 63.

[3] Fujii Y., K. Satake, S-I. Sakai, M. Shinohara, and T. Kanazawa (2011), Tsunami source of the 2011 off the Pacific coast of Tohoku, Japan earthquake, *Earth Planets Space*, 63.

[4] Gusman, A. R., Y. Tanioka, T. Kobayashi, H. Latief, and W. Pandoe (2010), Slip distribution of the 2007 Bengkulu earthquake inferred from tsunami waveforms and InSAR data, *J. Geophys. Res.*, 115, B12316, doi:10.1029/2010JB007565.

[5] Johnson, J. M. (1999), Heterogeneous coupling along Alaska-Aleutians as inferred from tsunami, seismic, and geodetic inversions, *Adv. Geophys.*, 39, 1-116.

[6] Kajiura, K. (1963), The leading wave of a tsunami, *Bulletin of the Earthquake Research Institute*, 41, 535-571.

[7] Lay, T., C. J. Ammon, H. Kanamori, L. Xue, and M. J. Kim (2011), Possible large near-trench slip during the great 2011 Tohoku (Mw 9.0) earthquake, *Earth Planets Space*, 63.

[8] Lawson, C. L. and B. J. Hanson (1974), Solving least squares problems, Prentice Hall, Inc., Englewood Cliffs, New Jersey, US.

[9] Maeda T., T. Furumura, S. Sakai, and M. Shinohara (2011), Significant tsunami observed at the ocean-bottom pressure gauges at 2011 the Pacific Coast of Tohoku Earthquake, *Earth Planets Space*, 63.

[10] Okada, Y. (1985), Surface deformation due to shear and tensile faults in half-space, *Bull. Seism. Soc. Am.*, 75-4, 1135-1154.

[11] Ozawa S., T. Nishimura, H. Suito, T. Kobayashi, M. Tobita, and T. Imakiire (2011), Coseismic and postseismic slip of the 2011 magnitude-9 Tohoku-Oki earthquake, *Nature*, 475, 373-376, doi:10.1038/nature10227.

[12] Sagiya, T., S. Miyazaki, and T. Tada (2000), Continuous GPS array and present-day crustal deformation of Japan, *Pure Appl. Geophys.*, 157, 2303-2322.

[13] Satake, K. (2002), Tsunamis, in *International Handbook of Earthquake and Engineering Seismology*, 81A, edited by W. H. K. Lee et al., pp. 437-451, Academic Press.

[14] Sato, M., T. Ishikawa, N. Ujihara, S. Yoshida, M. Fujita, M. Mochizuki, and A. Asada (2011), Displacement above the hypocenter of the 2011 Tohoku earthquake, *Science*, 1-2, doi:10.1126/science.1207401.

[15] Seno, T. (2000), The 21 September, 1999 Chichi earthquake in Taiwan: implications for tsunami earthquakes, *Terr. Atmos. Ocean Sci.*, 11, 701-708.

[16] Seno, T. and K. Hirata (2007), Did the 2004 Sumatra-Andaman earthquake involve a component of tsunami earthquakes?, *Bull. Seism. Soc. Am.*, 97-1A, S296-S306, doi:10.1785/0120050615.

[17] Synolakis, C. E., E. N. Bernard, V. V. Titov, U. Kanoglu, and F. I. Gonzalez (2008), Validation and verification of tsunami numerical models, *Pure Appl. Geophys.*, 165, 2197-2228, doi:10.1007/s00024-004-0427-y.

[18] Tanioka, Y. and T. Seno (2001), Sediment effect on tsunami generation of the 1896 Sanriku tsunami earthquake, *Geophys. Res. Lett.*, 28-17, 3389-3392.

[19] Yoshida, Y., H. Ueno, D. Muto, and S. Aoki (2011), Source process of the 2011 off the Pacific Coast of Tohoku earthquake with the combination of teleseismic and strong motion data, *Earth Planets Space*, 58, 1-5.